

# Structures of Organic Additives Modified Magnetite Nanoparticles

Yoshimitsu Kuwahara<sup>a</sup>, Toshiki Miyazaki<sup>a</sup>, Yuki Shirosaki<sup>b</sup>, Gengci Liu<sup>c</sup>  
and Masakazu Kawashita<sup>c</sup>

<sup>a</sup>*Graduate School of Life Science and System Engineering, Kyushu Institute of  
Technology, Kitakyushu, Japan*

<sup>b</sup>*Frontier Research Academy for Young Researchers, Kyushu Institute of Technology,  
Kitakyushu, Japan*

<sup>c</sup>*Graduate School of Biomedical Engineering, Tohoku University, Sendai, Japan*

## Corresponding author:

Toshiki Miyazaki

Graduate School of Life Science and Systems Engineering, Kyushu Institute of  
Technology, 2-4, Hibikino, Wakamatsu-ku, Kitakyushu 808-0196, Japan

Tel&Fax: +81-93-695-6025

Email: tmiya@life.kyutech.ac.jp

© 2016. This manuscript version is made available under the CC-BY-NC-ND 4.0 license  
<http://creativecommons.org/licenses/by-nc-nd/4.0/>

1           **Abstract**  
2

3           Magnetite (Fe<sub>3</sub>O<sub>4</sub>) nanoparticles and magnetite-based inorganic-organic hybrids  
4           are attracting increasing attention in biomedicine, as thermoseeds for hyperthermia and  
5           contrast media in magnetic resonance imaging. Controlling the size of Fe<sub>3</sub>O<sub>4</sub> thermoseeds  
6           is important, as particle size affects their heat generation under alternative magnetic fields.  
7           Fe<sub>3</sub>O<sub>4</sub> is easily synthesized via aqueous processes. We previously demonstrated that  
8           adding organic polymers during synthesis affected the size and crystallinity of the  
9           resulting Fe<sub>3</sub>O<sub>4</sub>. However, the relationship of the chemical structure of the  
10          low-molecular-weight organic additive of its effect on the product has not been  
11          elucidated. In this study, organic compounds containing varying functional groups and  
12          surface charges were added to the precursor solution of Fe<sub>3</sub>O<sub>4</sub>. Crystalline Fe<sub>3</sub>O<sub>4</sub> formed  
13          in the presence of neutral acetone, cationic ethylenediamine, and acetic acid. These  
14          nanoparticles had slightly smaller particle sizes than those prepared in the absence of  
15          additives. The presence of oxalic acid and tris(hydroxymethyl)aminomethane inhibited  
16          Fe<sub>3</sub>O<sub>4</sub> nucleation, instead yielding lepidocrosite- or akaganeite-type FeOOH. These  
17          differences were attributed to the ability to form complexes between iron ions and the  
18          organic additives. The saturation magnetizations of the products were consistent with  
19          Fe<sub>3</sub>O<sub>4</sub>. This indicated that the crystal phase of the iron oxide products differed, even when  
20          prepared in the presence of organic additives of the same functional group. It is concluded  
21          that state of ion-organic molecule complex in the solutions is a key factor governing  
22          nanostructure of the resultant iron oxide.  
23  
24  
25  
26  
27  
28  
29  
30  
31  
32  
33  
34  
35  
36  
37  
38  
39  
40  
41  
42  
43  
44  
45  
46  
47  
48  
49  
50

51          **Keywords:** A: Powders: chemical preparation, D: Ferrites, E: Biomedical applications  
52  
53  
54  
55  
56  
57  
58  
59  
60  
61  
62  
63  
64  
65

## 1. Introduction

Magnetite ( $\text{Fe}_3\text{O}_4$ ) is an inorganic material with applications in magnetism, electronics, and biomedicine. It shows promise for use in thermoseeds in cancer hyperthermia. Hyperthermia is a low-invasion cancer treatment, based on the lower heat resistivity of cancer cells compared with healthy cells [1]. Tumors can be heated by infrared radiation, radiofrequency ablation, and hot water treatment. However, tumors deep within the body cannot be effectively treated because these techniques require heating from outside the body. New cancer treatments using ferromagnetic ceramic particles such as  $\text{Fe}_3\text{O}_4$  and  $\gamma$ -hematite ( $\gamma\text{-Fe}_2\text{O}_3$ ) are attracting much attention. Deep tumors can be heated effectively and killed, if ferromagnetic ceramic particles are implanted around the tumors and an alternating magnetic field is applied. Various magnetic nanoparticles have been investigated as thermoseeds for this process [2,3]. Implanting 20–30  $\mu\text{m}$  size ferromagnetic microspheres in blood vessels around the tumors can result in hyperthermia and embolization effects, cutting off nutrient supply to the tumors [4–6].

We previously prepared  $\text{Fe}_3\text{O}_4$  nanoparticles by adding various water-soluble polymers. The nanoparticles size and crystal phase were controlled by the polymer structure and addition sequence [7].  $\text{Fe}_3\text{O}_4$  was formed by adding polystyrene sulfonate, rather than polyacrylic acid, so different iron oxides could be formed after adding the negatively charged polymer. The interaction between  $\text{Fe}_3\text{O}_4$  and small organic molecules is important in biomedicine, as many biomolecules such as amino acids and drugs are of low molecular weights. The crystal structure of iron oxide is reportedly controlled by complex formation upon adding ethylenediaminetetraacetic acid (EDTA) [8, 9].

1 However, the effect of adding organic molecules with different functional group has not  
2  
3 been comprehensively investigated.  
4

5  
6 In the present study, we synthesized Fe<sub>3</sub>O<sub>4</sub> nanoparticles in the presence of oxalic  
7  
8 acid, acetic acid, acetone, tris(hydroxymethyl)aminomethane, and ethylenediamine.  
9  
10 Their chemical structures are shown in Fig. 1. We investigated the effect of the additives  
11  
12 chemical structure on the crystalline phase, crystalline size, and magnetic properties of  
13  
14 the resulting nanoparticles.  
15  
16

## 17 18 19 20 21 **2. Materials and Methods**

22  
23 Oxalic acid, acetic acid, acetone, ethylenediamine, and iron (II) chloride were  
24  
25 purchased from Wako Pure Chemical Industries, Osaka, Japan.  
26  
27 Tris(hydroxymethyl)aminomethane was purchased from Nacalai Tesque, Kyoto, Japan.  
28  
29 Oxalic acid, acetic acid, acetone, tris(hydroxymethyl)aminomethane, or ethylenediamine  
30  
31 was dissolved in 25 mL of 1.2 mM aqueous iron (II) chloride at 4 mass%. Aqueous 1 M  
32  
33 NaOH was then added dropwise, until the pH was ~7. The resulting solution was stirred at  
34  
35 75°C for 1 h to precipitate solid particles. In the case of ethylenediamine, NaOH was not  
36  
37 added because the pH of the solution was already >7. The solution was then dialyzed by a  
38  
39 cellulose tube for 24 h to remove excessive water-soluble by-products, and the formed  
40  
41 precipitate was collected by filtration.  
42  
43  
44  
45  
46

47  
48 Crystalline structures were investigated using powder X-ray diffraction (XRD,  
49  
50 MXP3V, Mac Science Ltd., Yokohama, Japan). The size and shape of the products were  
51  
52 observed using transmission electron microscopy (TEM, JEM-3010, JEOL, Tokyo,  
53  
54 Japan). The saturation magnetizations of the samples were measured using vibrating  
55  
56  
57  
58  
59  
60  
61  
62  
63  
64  
65

1 sample magnetometry (VSM, VSM-5, Toei, Tokyo, Japan), under an applied magnetic  
2  
3 field (10 kOe, 80 Hz).  
4  
5  
6  
7

### 8 **3. Results and Discussion**

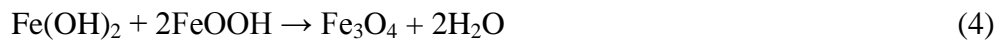
9

10 Figure 2 shows the XRD patterns of the samples. Peaks characteristic of  
11 crystalline Fe<sub>3</sub>O<sub>4</sub> (JCPDS#19-0629) were apparent for samples prepared with no additive,  
12  
13 acetic acid, acetone, and ethylenediamine. Peaks characteristic of lepidocrocite-type  
14  
15 FeOOH (JCPDS#44-1415) and akaganeite-type FeOOH (JCPDS#34-1266) were  
16  
17 detected in the patterns of samples prepared with oxalic acid and  
18  
19 tris(hydroxymethyl)aminomethane, respectively.  
20  
21  
22  
23  
24

25 Figure 3 shows TEM images and particle size histograms of the samples. Cubic  
26  
27 particles were observed for samples prepared with no additive, acetone, ethylenediamine,  
28  
29 and acetic acid. The average particle sizes of samples prepared in the presence of organic  
30  
31 additives was slightly smaller than the sample prepared with no additive. Fine particles of  
32  
33 3 nm in size were observed for the sample prepared with oxalic acid. Needle-like particles  
34  
35 larger than 200 nm were observed for the sample prepared with  
36  
37 tris(hydroxymethyl)aminomethane.  
38  
39  
40  
41

42 Table 1 shows the saturation magnetizations of the samples, and whether or not  
43  
44 Fe<sub>3</sub>O<sub>4</sub> was formed. The samples containing crystalline Fe<sub>3</sub>O<sub>4</sub> exhibited high saturation  
45  
46 magnetizations of 40–57 emu/g, in the order: acetone > no additive > acetic acid >  
47  
48 ethylenediamine. Samples not containing crystalline Fe<sub>3</sub>O<sub>4</sub> exhibited lower saturation  
49  
50 magnetizations.  
51  
52  
53  
54  
55  
56  
57  
58  
59  
60  
61  
62  
63  
64  
65

1           These results indicated that the crystal phase of the prepared iron oxide  
2  
3 nanoparticles was sensitive to the organic additive. Fe<sub>3</sub>O<sub>4</sub> forms by reaction of the Fe<sup>2+</sup>  
4 and Fe<sup>3+</sup> precursors according to [10, 11]:  
5  
6  
7  
8  
9



14  
15  
16  
17  
18  
19  
20  
21  
22  
23           A strong interaction was thought to form between the iron ions and the organic  
24 additive functional groups, yielding a complex. A significant amount of Fe<sup>2+</sup> within the  
25 complex was oxidized by O<sub>2</sub> gas dissolved from surrounding air, so insufficient Fe<sup>2+</sup> was  
26 present for Fe<sub>3</sub>O<sub>4</sub> formation.  
27  
28  
29  
30  
31

32           Samples prepared in the presence of acetic and oxalic acids showed different  
33 results, despite both possessing carboxyl group. Stability of complex is discussed in terms  
34 of stability constants. When metal ion M reacts with ligand L to form a complex ML, the  
35 stability constant K is expressed as follows:  
36  
37  
38  
39  
40  
41



$$43 \quad K = \frac{[\text{ML}]}{[\text{M}][\text{L}]} \quad (6)$$

44  
45  
46  
47  
48  
49           The stability constants of the Fe(COO)<sub>2</sub> and Fe(CH<sub>3</sub>COO)<sup>2+</sup> complexes are  
50 reportedly 10<sup>7.53</sup> and 10<sup>3.38</sup>, respectively [12, 13]. Thus, the iron-oxalic acid complex was  
51 more stable than the iron-acetic acid complex, so oxalic acid more strongly inhibited  
52 Fe<sub>3</sub>O<sub>4</sub> formation.  
53  
54  
55  
56  
57  
58  
59  
60  
61  
62  
63  
64  
65

1 Ethylenediamine and tris(hydroxymethyl)aminomethane both contain the cationic  
2 amino group, but yielded different iron oxides. Two molecules of  
3 tris(hydroxymethyl)aminomethane were thought to complex with one iron ion (Fig. 4),  
4 which inhibited Fe<sub>3</sub>O<sub>4</sub> nucleation [14]. Fe<sub>3</sub>O<sub>4</sub> nanoparticles were formed, despite  
5 ethylenediamine being able to complex with iron ions (stability constant = 10<sup>4.3</sup>). The pH  
6 of the solution immediately increased to 10 after adding ethylenediamine, while the pH  
7 was ~6 after adding tris(hydroxymethyl)aminomethane. It was thought that Fe(OH)<sub>2</sub>  
8 formed as a precursor to Fe<sub>3</sub>O<sub>4</sub>, immediately after adding ethylenediamine.  
9

10 We previously reported that Fe<sub>3</sub>O<sub>4</sub> formed in the presence of cationic  
11 poly(diallyldimethylammonium chloride) (PDDAC) [7]. Fe<sub>3</sub>O<sub>4</sub> formation clearly differs  
12 in the presence of low- and high-molecular-weight organic additives, even when their  
13 charges are similar. PDDAC does not contain functional group that can act as a ligand, so  
14 PDDAC and iron did not significantly interact, which did not inhibit Fe<sub>3</sub>O<sub>4</sub> formation.  
15

16 Samples containing crystalline Fe<sub>3</sub>O<sub>4</sub> exhibited much higher saturation  
17 magnetizations than those containing FeOOH (Table 1). Li *et al.* evaluated the magnetic  
18 properties of Fe<sub>3</sub>O<sub>4</sub> nanoparticles of size 8–43 nm [15]. Those of 8 nm in size exhibited a  
19 saturation magnetization of 67.3 emu/g. Kucheryavy *et al.* prepared nanoparticles of size  
20 3.2–7.5 nm, by heating a solution of iron chloride in diethylene glycol. The saturation  
21 magnetization decreased with decreasing particle size [16]. The present results show a  
22 similar trend. Thus, the magnetic properties can be controlled by modifying with organic  
23 additives containing different structures.  
24

#### 25 4. Conclusions

26  
27  
28  
29  
30  
31  
32  
33  
34  
35  
36  
37  
38  
39  
40  
41  
42  
43  
44  
45  
46  
47  
48  
49  
50  
51  
52  
53  
54  
55  
56  
57  
58  
59  
60  
61  
62  
63  
64  
65

1 Iron oxide nanoparticles were prepared in aqueous solution in the presence of  
2  
3 various organic additives. The nanoparticles size and crystal phase were significantly  
4  
5 affected by the organic additive. Additives able to form complexes tended to inhibit  
6  
7  $\text{Fe}_3\text{O}_4$  formation. The interaction between iron ions and additive functional group acted as  
8  
9 a precursor, and affected the crystal structure of the product. These results aid our  
10  
11 knowledge on preparing  $\text{Fe}_3\text{O}_4$  nanoparticles modified with organic substances for  
12  
13 different magnetic properties.  
14  
15  
16  
17  
18  
19

## 20 **Acknowledgments**

21  
22 This study was supported by a Grant-in-Aid for Scientific Research on Innovative Areas,  
23  
24 “Fusion Materials: Creative Development of Materials and Exploration of Their Function  
25  
26 through Molecular Control” (No. 2206) from the Ministry of Education, Culture, Sports,  
27  
28 Science and Technology, Japan.  
29  
30  
31  
32  
33

## 34 **References**

- 35  
36  
37 [1] J. Conway, A.P. Anderson, Electromagnetic techniques in hyperthermia. Clin. Phys.  
38  
39 Physiol. Meas. 7 (1986) 287-318.  
40  
41  
42 [2] B. Jeyadevan, Present status and prospects of magnetite nanoparticles-based  
43  
44 hyperthermia. J. Ceram. Soc. Jpn. 118 (2010) 391-401.  
45  
46  
47 [3] T. Kobayashi, T. Cancer hyperthermia using magnetic nanoparticles. Biotechnol. J.  
48  
49 6 (2011) 1342-1347.  
50  
51  
52 [4] E. Day, Radiotherapy glasses, In: L.L. Hench, J. Wilson (Eds.), An Introduction to  
53  
54 Bioceramics, World Scientific, Singapore, 1993, pp. 305-317.  
55  
56  
57  
58  
59  
60  
61  
62  
63  
64  
65



- 1 [5] M. Kawashita, Ceramic microspheres for biomedical applications. *Int. J. Appl.*  
2  
3  
4 *Ceram. Technol.* 2 (2005) 173-183.  
5
- 6 [6] T. Miyazaki, A. Miyaoka, E. Ishida, Z. Li, M. Kawashita, M. Hiraoka, Preparation  
7  
8 of ferromagnetic microcapsules for hyperthermia using water/oil emulsion as a  
9  
10 reaction field. *Mater. Sci. Eng., C* 32 (2012) 692-696.  
11
- 12 [7] Y. Kuwahara, T. Miyazaki, Y. Shirosaki, M. Kawashita, Effects of organic polymer  
13  
14 addition in magnetite synthesis on the crystalline structure, *RSC Adv.*, 4 (2014)  
15  
16 23359-23363.  
17
- 18 [8] Y. Oaki, N. Yagita, H. Imai, One-pot aqueous solution syntheses of iron oxide  
19  
20 nanostructures with controlled crystal phases through a  
21  
22 microbial-mineralization-inspired approach, *Chem. Eur. J.*, 18 (2012) 110–116.  
23  
24
- 25 [9] N. Yagita, Y. Oaki, H. Imai, A microbial-mineralization approach for syntheses of  
26  
27 iron oxides with a high specific surface area. *Chem. Eur. J.*, 19 (2013) 4419-4422.  
28  
29
- 30 [10] S. Lian, E. Wang, Z. Kang, Y. Bai, L. Gao, M. Jiang, C. Hu, L. Xu, Synthesis of  
31  
32 magnetite nanorods and porous hematite nanorods. *Solid State Commun.* 129 (2004)  
33  
34 485-490.  
35  
36
- 37 [11] M. Mahmoudi, A. Simchi, M. Imani, A.S. Milani, P. Stroeve, Optimal design and  
38  
39 characterization of superparamagnetic Iron Oxide nanoparticles coated with  
40  
41 polyvinyl alcohol for targeted delivery and imaging. *J. Phys. Chem. B* 112 (2008)  
42  
43 14470-14481.  
44  
45  
46  
47  
48
- 49 [12] A.E. Martell, R.M. Smith, *Critical Stability Constants*, Plenum Press, New York,  
50  
51 1975.  
52  
53  
54  
55  
56  
57  
58  
59  
60  
61  
62  
63  
64  
65

- 1 [13] Y. Kanroji, Studies on the complex ions in mineral springs. II. stability constants of  
2 iron (III) sulfate and chloride complexes, *Yakugaku Zasshi* 83 (1963) 424-427 (in  
3 Japanese).  
4  
5  
6  
7  
8 [14] R.L. Dotson, Characterization and studies of some four, five and six coordinate  
9 transition and representative metal complexes of  
10 tris-(hydroxymethyl)-aminomethane, *J. Inorg. Nucl. Chem.*, 34 (1972) 3131–3138.  
11  
12  
13 [15] Z. Li, M. Kawashita, N. Araki, M. Mitsumori, M. Hiraoka, M. Doi, Magnetite  
14 nanoparticles with high heating efficiency for application in hyperthermia of cancer,  
15 *Mater. Sci. Eng. C*, 30 (2010) 990-996.  
16  
17  
18 [16] P. Kucheryavy, J. He, V.T. John, P. Maharjan, L. Spinu, G.Z. Goloverda, V.L.  
19 Kolesnichenko, Superparamagnetic Iron Oxide Nanoparticles with Variable Size  
20 and an Iron Oxidation State as Prospective Imaging Agents, *Langmuir* 29 (2013)  
21 710–716.  
22  
23  
24  
25  
26  
27  
28  
29  
30  
31  
32  
33  
34  
35  
36  
37  
38  
39  
40  
41  
42  
43  
44  
45  
46  
47  
48  
49  
50  
51  
52  
53  
54  
55  
56  
57  
58  
59  
60  
61  
62  
63  
64  
65

**Table 1.** Sample saturation magnetizations and Fe<sub>3</sub>O<sub>4</sub> formation.

Organic additive	Magnetite formed	Saturation Magnetization (emu/g)
None	Yes	57.07
Oxalic acid	No	2.61
Acetic acid	Yes	48.33
Acetone	Yes	57.84
Tris(hydroxymethyl) aminomethane	No	0.62
Ethylenediamine	Yes	39.96

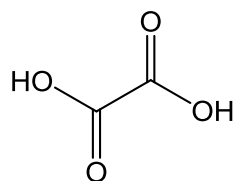
1 **Figure captions**  
2  
3  
4  
5

6 **Fig. 1.** Chemical structures of organic reagents.  
7

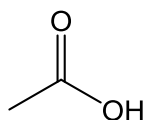
8 **Fig. 2.** XRD patterns of samples prepared in the presence of organic additives.  
9

10 **Fig. 3.** TEM images and particle size distributions of samples prepared in the presence of  
11 organic additives.  
12  
13  
14

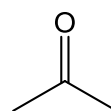
15 **Fig. 4.** Complex formed between iron and tris (hydroxymethyl) aminomethane.  
16  
17  
18  
19  
20  
21  
22  
23  
24  
25  
26  
27  
28  
29  
30  
31  
32  
33  
34  
35  
36  
37  
38  
39  
40  
41  
42  
43  
44  
45  
46  
47  
48  
49  
50  
51  
52  
53  
54  
55  
56  
57  
58  
59  
60  
61  
62  
63  
64  
65



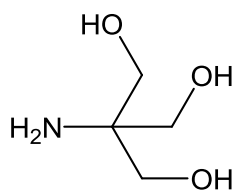
Oxalic acid



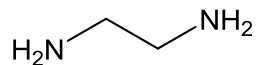
Acetic acid



Acetone



Tris(hydroxymethyl)  
aminomethane



Ethylenediamine

**Fig. 1.** Chemical structures of organic reagents.

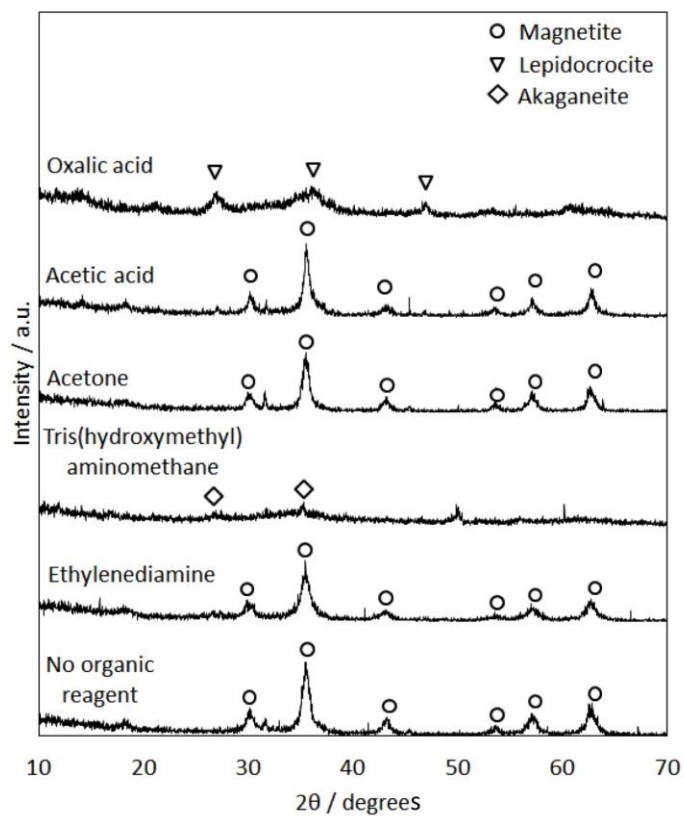


**Fig. 2.** XRD patterns of samples prepared in the presence of organic additives.

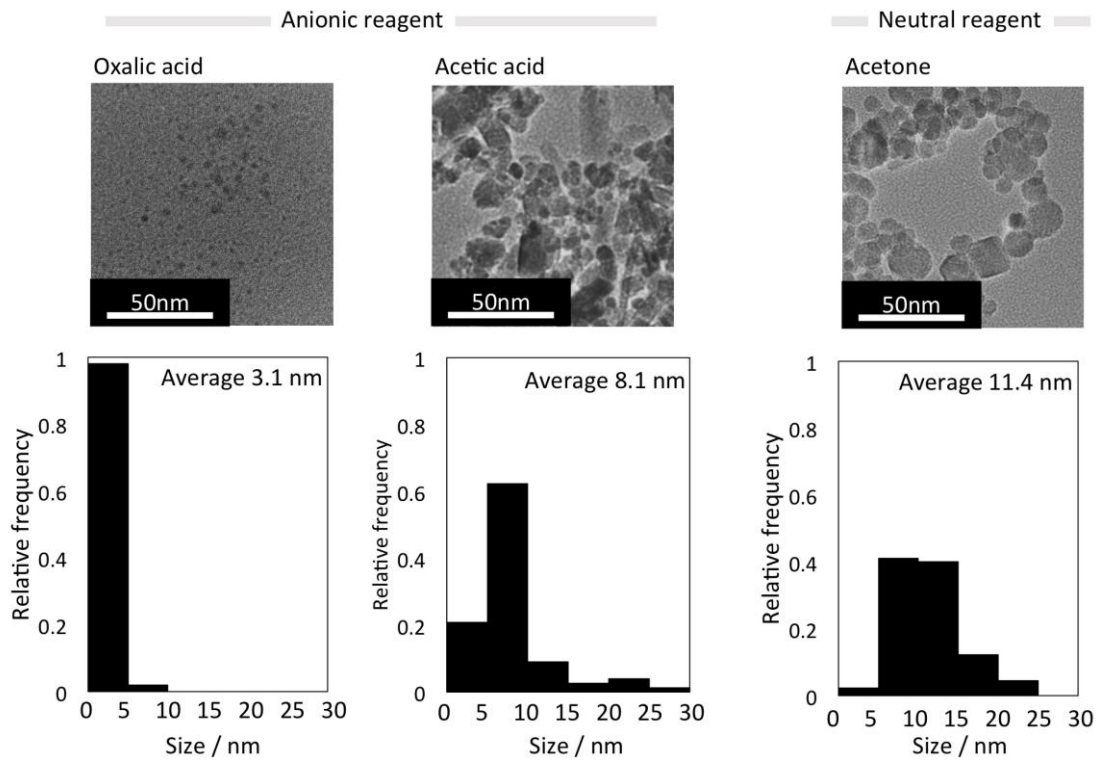


**Fig. 3.** TEM images and particle size distributions of samples prepared in the presence of organic additives.

1  
2  
3  
4  
5  
6  
7  
8  
9  
10  
11  
12  
13  
14  
15  
16  
17  
18  
19  
20  
21  
22  
23  
24  
25  
26  
27  
28  
29  
30  
31  
32  
33  
34  
35  
36  
37  
38  
39  
40  
41  
42  
43  
44  
45  
46  
47  
48  
49  
50  
51  
52  
53  
54  
55  
56  
57  
58  
59  
60  
61  
62  
63  
64  
65

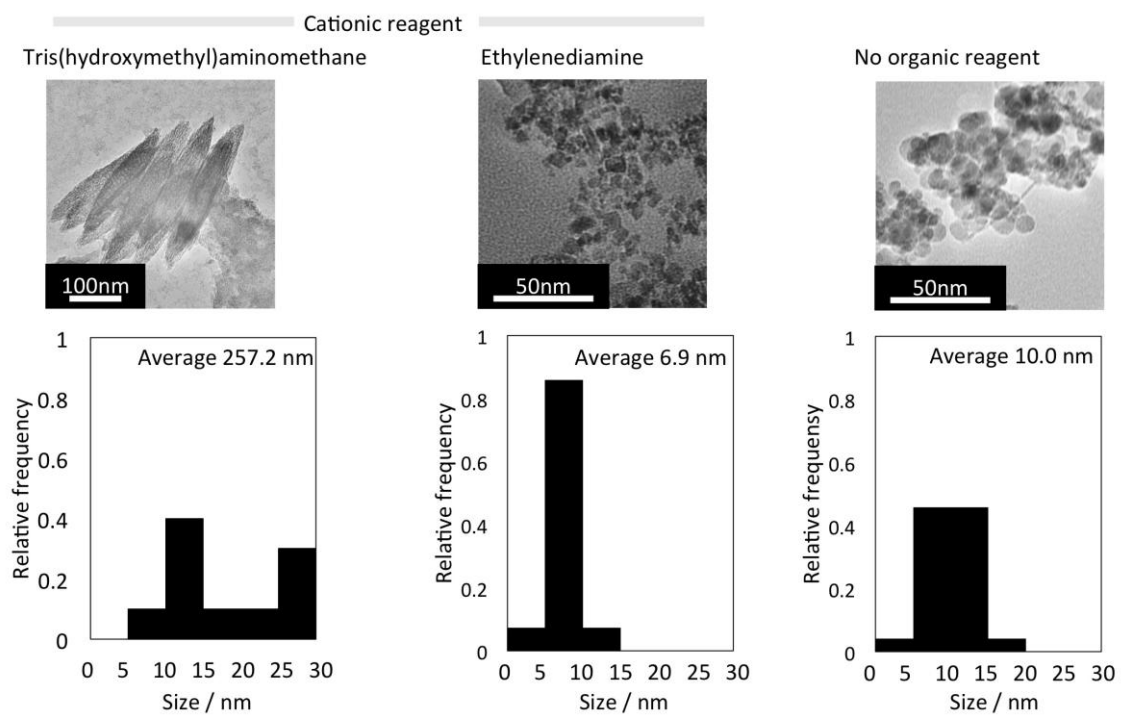


**Fig. 3. (Continued)**



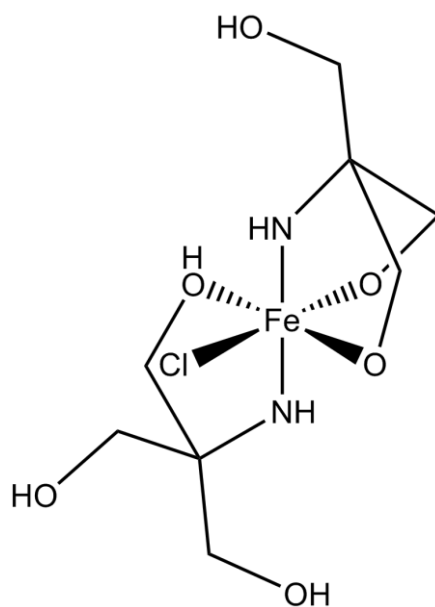


**Fig. 4.** Complex formed between iron and tris (hydroxymethyl) aminomethane.